

Remaining useful life prediction of lithium-ion batteries via an EIS based deep learning approach

Jie Li ^a, Shiming Zhao ^a, Md Sipon Miah ^{a,b,c}, Mingbo Niu ^{a,*}

^a Internet of Vehicle to Road Low-Carbon Research Institute, Chang'an University, Shaanxi 710064, China

^b Department of Signal Theory and Communications, Universidad Carlos III de Madrid, Leganés, 28911 Madrid, Spain

^c Department of Information and Communication Technology, Islamic University, Kushtia, 7003, Bangladesh



ARTICLE INFO

Keywords:

Deep learning
Electrochemical impedance spectroscopy
Lithium batteries
Remaining useful life

ABSTRACT

Reliable life prediction technology is of great significance in ensuring a safe and efficient lifetime of lithium batteries. However, the traditional health factors such as battery capacity are the effects of battery aging rather than the direct causes, which cannot directly reflect the internal degradation mechanism information of the battery, and the prediction accuracy is easily affected by the working environment of the battery. Electrochemical impedance spectroscopy (EIS) data can more directly reflect the internal mechanism information of the battery, which includes a wealth of battery aging information. In order to deeply investigate the mapping relationship between impedance spectrum and remaining useful life (RUL) of lithium batteries, EIS method is employed to obtain the impedance and phase of lithium batteries under different health states and temperatures, as well as explore the visualization and quantification of impedance frequency response of lithium battery. Furthermore, the mapping relationship between RUL and the lithium battery impedance is investigated in a full impedance spectrum at different temperatures. It is found that, as lithium battery aging, its negative imaginary parts impedance increases significantly, especially in the middle of the frequency band, and has no significant dependence on temperature. While the real part impedance shows an obvious dependence on temperature. Therefore, it is found that the negative imaginary parts impedance of impedance spectrum has a well-fit characterization ability for RUL of a lithium battery. In this paper, a fusion neural network model of Conv1d-SAM (one-dimensional convolutional neural network-self-attention mechanism) was established with negative imaginary part impedance as input factor to predict battery RUL. The predicted results show that Conv1d-SAM has improved accuracy and stability in RUL prediction, and the mean absolute error function of the proposed model is increased by 72% compared with the latest published method.

1. Introduction

Lithium batteries are widely used in various fields due to their high energy density, light-weight, long cycle life, and environmental friendliness (Wang and Mamo, 2018; Xia et al., 2018). During the operation of lithium-ion batteries, some irreversible chemical reactions will occur inside the battery, resulting in increase of internal resistance and performance degradation (Guha and Patra, 2018). Therefore, reliable life prediction technology is not only important for the efficient use of batteries, but also reduces their failure rate. In recent years, as a key technology for lithium-ion battery management, assurance and predictive maintenance, remaining useful life (RUL) has attracted much attention and developed into one of the hot issues in electronic system

failure prediction and health management technology research (Dong et al., 2018; Zhou et al., 2019).

RUL prediction is mainly to predict the remaining usage times of the battery according to the battery current state. The existing lithium battery life prediction methods can be mainly divided into physical equivalent model, electrochemical model and data-driven methods (Li and Yang, 2020; Chen et al., 2020). The first two can be classified as physical models, which are mainly based on electrochemical mechanism (Ramadas et al., 2003), electrochemical impedance spectroscopy (Zhu et al., 2015) or equivalent circuit model (Hu et al., 2012). Reference (Zou et al., 2016) established the state space model of the electrochemical battery based on the constant phase element of non-integer order derivative. The model could accurately predict the health state

* Corresponding author.

E-mail address: ivr.niu@chd.edu.cn (M. Niu).

of the battery by combining the electrochemical impedance spectrum and impedance coefficient. References (Yang et al., 2018) through the analysis of the time constant of constant-voltage charging current and battery aging correlation, established the first order equivalent circuit model (ECM). Reference (Saha et al., 2009) designed an equivalent circuit model, which can simulate the working process of the battery. Finally, the correlation vector machine algorithm and particle filter method were integrated to realize the prediction of the remaining life of the battery. Reference (Guha and Patra, 2018) established a model of battery internal resistance growth based on electrochemical impedance spectroscopy (EIS) test data, and used this model to estimate the remaining useful life of the battery. The above literature realizes the prediction of battery RUL by establishing electrochemical model and equivalent circuit model, and expounds the feasibility of model prediction method. However, due to the battery works in different working conditions, the physical characteristics of the battery itself is also change to a certain extent, which is greatly affected by external conditions. Therefore, it is difficult to fully grasp the working mechanism and process of lithium batteries, thus the accuracy of RUL prediction is unsatisfactory. The data-driven method extracts the life information contained in the lithium battery degradation data, it employs the big data method to learn the internal laws from the degradation data, and establishes a data-driven mathematical model to predict RUL. It does not need to fully grasp the working mechanism of the lithium battery itself, and the prediction accuracy can be significantly improved. It has become a research hotspot in the field of current lithium battery life prediction (Li et al., 2019; Deng et al., 2020).

The challenge of data-driven models, however, lies in obtaining informative inputs to build robust models for predicting battery characteristics. Furthermore, effectively extracting features from historical data is still a challenging task (Li and Yang, 2020; Chen et al., 2020; Babaeiyazdi et al., 2021). Reference (Xiong et al., 2019) extracted the health index according to the partial charging voltage curve of the battery, and used the linear aging model constructed based on the capacity data in the moving window to predict the remaining service life of the battery. Reference (Sun et al., 2018) used the particle filter algorithm to predict RUL according to the third-order polynomial model. Reference (Shen et al., 2019) employed capacity as the health indicator to characterize the degradation of lithium-ion batteries, and proposed a stochastic model-based method for RUL predicting. Reference (Sun et al., 2019) proposed a hybrid method for predicting battery RUL based on particle filter (PF) and extreme learning machine (ELM). Reference (Wu et al., 2017) established an indirect prediction model for RUL prediction based on the indirect health coefficient method of the discharge voltage difference at equal time intervals. Reference (Zhou et al., 2020) took the capacity of the battery degradation process as a feature, and proposed an attention mechanism-based convolutional neural network (CNN) and a position-encoding model for RUL prediction. Reference (Sun et al., 2023) established a hybrid model composed of multi-physics field simulation and Long Short-Term memory (LSTM) neural network, and integrated the simulation results obtained by the physical model into the LSTM network, so that it could dynamically update the prediction results obtained by the model and improve the ability of the model to predict battery SOH for a long time. These existing data-driven methods mostly used factors such as battery capacity, voltage difference, and equal-voltage charging time to predict RUL of lithium batteries, however, although factors described above show a certain correlation with RUL, changes of these factors are the effect rather than the cause of battery aging. Therefore, the accuracy and stability of prediction based on data driven methods are greatly limited.

The electrochemical impedance spectroscopy (EIS) method provides a non-destructive method to comprehensively understand the electrochemical reaction kinetics and an aging mechanism of lithium ions, and the system impedance spectroscopy test in a wide frequency range can obtain more than other conventional electrochemical methods. Kinetics, electrode interface structure, and electrochemical reaction information,

which contains impedance information over a wide frequency range, enables simultaneous characterization of different physicochemical processes reference (Zhang et al., 2020). Reference (Pastor-Fernández et al., 2016) studied EIS technology and proposed a method to identify and quantify the aging mechanism over time in essence, and the results showed that the loss of active material (LAM) and lithium ions are the fundamental of battery aging, the loss of active materials and lithium ions causes the impedance of the battery to increase, and resulting in battery aging. Meanwhile, reference (Messing et al., 2021) shows that impedance spectroscopy can provide basic information on the general state of the battery, and reference (Xiong et al., 2019) shows that the performance degradation of lithium batteries is mainly manifested by capacity loss and impedance increase, which is caused by side reactions, electrolyte decomposition, self-discharge and current collectors. Degradation caused by the literature of reference (Vetter et al., 2005; Birk et al., 2017; Broussely et al., 2005; Bohlen et al., 2007), also confirmed the above point of view.

Studies have shown that EIS applies voltage or current signals to the battery at different frequencies, and converts the response signal from the time domain to the frequency domain through Fourier transform, thereby obtaining a complete impedance spectrum inside the battery. The Nyquist plot of the impedance spectrum shows features corresponding to the internal impedance of the battery (Messing et al., 2020). Reference (Murariu and Morari, 2019) collects the impedance data of the battery in two states of charge through the EIS method, builds an equivalent circuit and successfully predicts the battery life. Reference (Agudelo et al., 2019) used EIS data to build an equivalent model to predict the state of health (SOH) of batteries. To sum up, the existing researches using EIS to predict the RUL of lithium batteries mainly rely on the qualitative interpretation of the parameters of the Nyquist plot, and the determination of RUL directly by impedance value or spectrum has not been in-depth investigated. However, some studies have confirmed that the change of the lithium battery impedance is enough to map its remaining available capacity, the impedance value increases linearly with the capacity decay of the lithium battery, and the impedance value changes with the degree of use of the battery and the frequency of impedance measurement (Murariu and Morari, 2019; Monika et al., 2018).

In order to deeply study the mapping relationship between EIS data and RUL, a method for predicting RUL of lithium battery based on EIS data is explored. EIS method can more directly obtain the internal mechanism information of the battery, which enables it to better map the battery RUL, therefore, In this paper, the EIS method is used to obtain the impedance magnitude and phase of the lithium battery under different health states and temperatures, and after the Fourier transform of the impedance information, it is converted into the real part of the impedance and negative imaginary part impedance imaginary part, the Nyquist diagram of the impedance map is generated, and the visualization and quantification of the impedance frequency response of the lithium battery is realized. Furthermore, the mapping relationship between RUL and lithium battery impedance was studied in the full impedance spectrum at different temperatures. The mapping relationship shows that as the lithium battery ages, its negative imaginary part impedance imaginary part increases significantly, especially in the mid-frequency band. Moreover, the real part impedance shows a significant dependence on battery temperature. In addition, the above conclusions are verified by Pearson correlation analysis. Based on the EIS method, this paper obtains the impedance data of lithium batteries at 60 measurement frequencies. Then a fusion model based on CNN and self-attention mechanism (SAM) is developed, and lithium battery aging features are extracted from impedance data. Furthermore, multilayer perceptron (MLP), one-dimensional convolutional neural network (Conv1d), two-dimensional convolutional neural network (Conv2d) are designed as competition models, and a detailed comparative study with the existing methods is carried out. The main contributions of this work are as follows:

1) The change rule of the real and negative imaginary parts impedance of the lithium battery with the aging at different working temperatures was studied, and it was clarified that in the full impedance spectrum, with the aging of the lithium battery at different temperatures, the relationship between RUL and real and negative imaginary parts impedance was determined mapping relations. The research results show that with the aging of the lithium battery, the negative imaginary part impedance increases significantly, especially in the middle frequency band, and has no significant dependence on temperature, while the real part impedance shows a significant dependence on the battery temperature. Through further quantitative analysis, it is found that the imaginary part of the lithium battery impedance spectrum has a good ability to characterize the RUL of the lithium battery.

2) The relationship between the imaginary part of the electrochemical impedance spectrum and the RUL of the lithium battery was established. Taking the amplitude-frequency characteristics of the imaginary part of the EIS impedance of the lithium battery as the input factor, Conv1d-SAM was designed and then the EIS-IM-Conv1d-SAM (Electrochemical impedance spectroscopy- negative imaginary part-one-dimensional convolutional neural network-self attention) model was constructed. The model can be used to estimate RUL of lithium batteries at different operating temperatures without using historical charge-discharge cycle data of lithium batteries.

3) MLP, Conv1d, Conv2d are considered as competitive models, and a detailed comparative study with existing methods is carried out, which confirms the superiority of the proposed method. The proposed method is superior to the competition models in terms of prediction accuracy and stability, and compared with the existing EIS-GPR method, the prediction accuracy is improved by 72% on average of the 9 cells studied.

The rest of this article is arranged as follows: Section I introduces the correlation analysis of EIS data and RUL; Section II presents the lithium battery remaining life prediction model Conv1d-SAM; Section III validates the proposed Conv1d-SAM by testing EIS impedance data, the effectiveness and superiority of the Conv1d-SAM model for predicting the RUL of lithium batteries is demonstrated by comparison with four competing models; Section IV concludes the paper.

2. EIS method

The EIS method, known as the AC impedance method, is an important means to study the electrochemical reactions and electrode interface phenomena of lithium batteries. A deeper understanding of the electrochemical process of lithium batteries can be obtained through EIS technology (Babaeiyazdi et al., 2021). The EIS method measures the battery response (i.e., voltage in the case of galvanostatic or current in the case of potentiostatic) by applying sinusoidal signals of different frequencies of current (galvanostatic) or voltage (potentiostatic) to the battery, and calculates the battery response. The magnitude and phase of the impedance are obtained. Meanwhile the real part and the negative imaginary part of the impedance is obtained after Fourier transform, so as to generate the Nyquist diagram (impedance spectrum) of the impedance map, according to which the active reaction of the lithium battery can be analyzed mechanism. The Nyquist plot enables the quantification and visualization of the frequency response of the battery, and contains information on the correlation of real and negative imaginary parts impedance with RUL of the battery. The impedance spectrum obtained by the EIS experiment in this paper is shown in Fig. 1. In Fig. 1, the horizontal axis represents the battery real part impedance, and the vertical axis represents the negative imaginary part impedance. The specific electrochemical process of the lithium battery can be divided into three types: high frequency (greater than 1 kHz), intermediate frequency (1~999 Hz) and low frequency (less than 1 Hz) according to the frequency part (Deng et al., 2020).

Notably, different regions of the impedance spectrum correspond to different chemical and physical processes taking place in the battery.

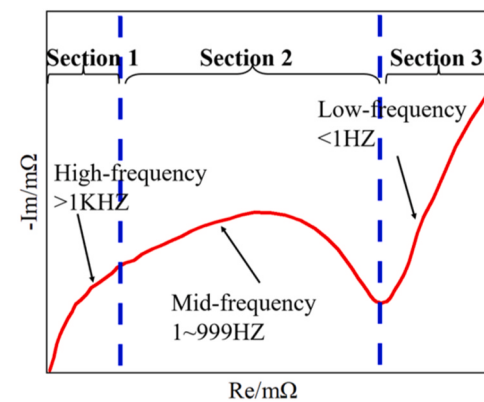


Fig. 1. EIS impedance spectrum.

The high frequency response is related to the inductive reactance of the metallic elements in the battery. Cell resistance represents the sum of current collector, active material, electrolyte and separator resistances. The mid-frequency response is semicircular, representing the double-layer capacitance on the electrode and the capacitance and resistance of the solid electrolyte interface (SEI) layer. The low-frequency response is ideally a curve with a constant slope, mainly showing the diffusion process of the electrode active material (Agudelo et al., 2019).

In this paper, the EIS method is used to analyze the whole aging process of nine lithium batteries at three temperatures (25 °C, 35 °C and 45 °C). Impedance spectra during battery aging at different states of health (SOH) and different temperatures can be obtained. The experimental subjects were nine 45 mA EunicellLR2032 lithium batteries, and data were collected in a constant current-constant voltage (CC-CV) cycle. Each measurement cycle consists of two steps, the first step is to charge the battery with CC-CV at a rate of 1 C (45 mA), and thus the battery reaches the rated voltage of 4.2 V, and then let it stand for 15 min. The second step was to discharge to 3 V at a constant current (CC) rate of 2 C (90 mA). When the frequency range is 0.02 Hz-20 kHz, EIS experiments were performed at 9 different stages of each even-numbered charge-discharge cycle. The 9 stages are: I: Before charging; II: Start charging; III: After 20 min charging; IV: After charging and before resting; V: After 15 min rest; VI: Start discharging; VII: After 10 min discharging; VIII: After discharging and before resting; IX: After 15 min rest.

The battery impedance information obtained by the EIS method apparently has a direct link to the RUL (Eddahch et al., 2012). Based on the experimental data, the relationship between RUL and EIS impedance spectrum is further clarified. The experimental data used in this article is from literature (Zhang et al., 2020), for detailed information on the experimental process, parameter settings and equipment list, please refer to literature (Zhang et al., 2020).

2.1. Analysis of the mapping relationship between RUL and EIS impedance

For an easy representation on battery number, 9 batteries used in the experiment are numbered as: 25-1, 25-2, 25-3, 25-4, 25-5, 35-6, 35-7, 45-8, 45-9, respectively, in which the first number represents the ambient temperature during the battery aging experiment, and the second number represents the serial number of these batteries. Fig. 2(a)-(c) shows the partial impedance spectra of 25-4, 35-7, 45-9, 0, 25%, 50%, 75% and 100% marked in Fig. 2 indicate that the maximum capacity of the battery is reduced by 0% of the rated state (factory state, 0 times of charge and discharge), 25%, 50%, 75% and greater than 80%, respectively. The maximum capacity of lithium batteries is often used to characterize RUL, thus the decrease in maximum capacity was used to map the decrease in RUL in this study.

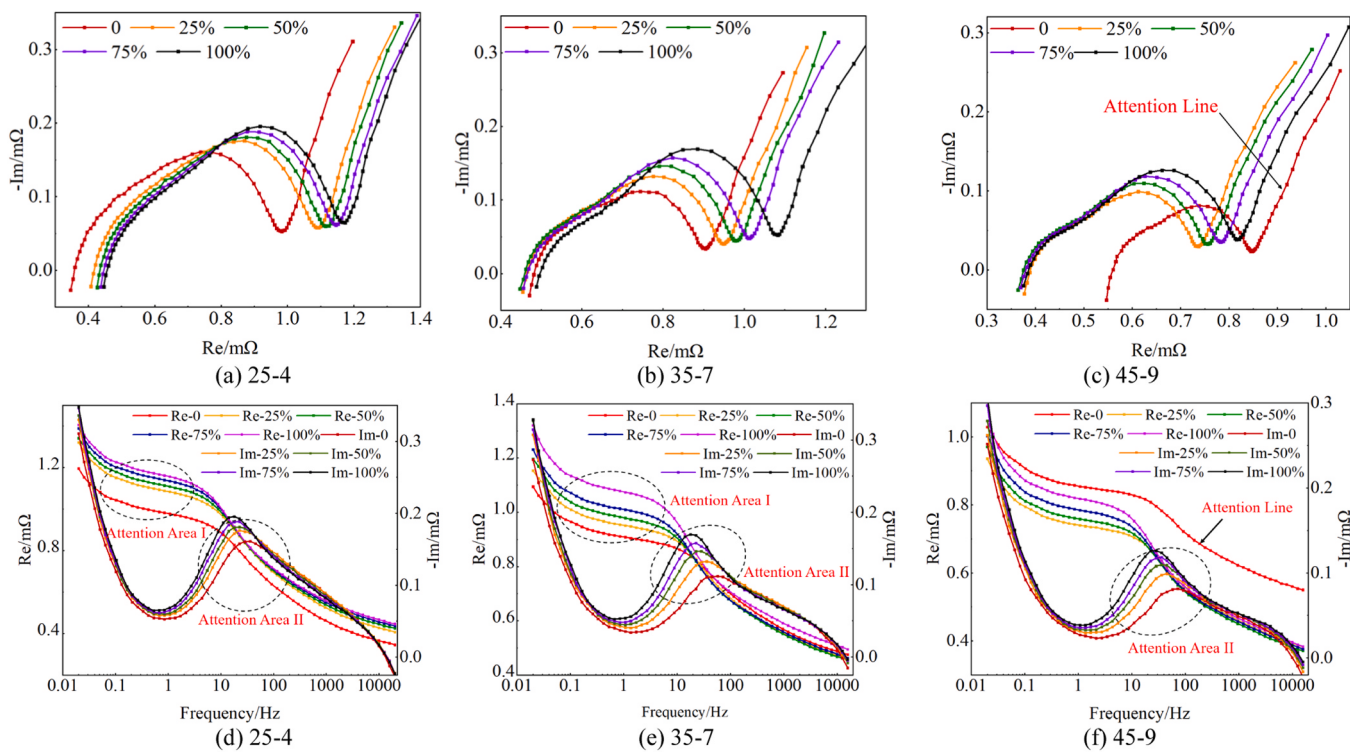


Fig. 2. Lithium battery aging test results at full frequency.

In this paper, the impedance spectra of lithium batteries at 25 °C, 35 °C, and 45 °C were investigated to explore the characteristics of real and negative imaginary parts impedance with the change of RUL at different temperatures. When the measurement frequency of the EIS method is 2 Hz, the EIS experiment is carried out on 9 batteries, and the test results of 3 batteries (25-4, 35-7 and 45-9) are selected to draw the impedance spectrum, as shown in Fig. 2(a)-(c). Furthermore, the changes of real and negative imaginary parts impedance in the EIS impedance data of 3 batteries under 60 measurement frequencies are shown in Fig. 2(d)-(e), where the abscissa represents the 60 test frequencies and the ordinate represents the battery real and negative imaginary parts impedance.

It can be seen from Fig. 2(a)-(c) that at different temperatures, as the RUL decreases (that is, the maximum capacity of the lithium battery decreases), the basic change rule of the impedance spectrum is that the intermediate frequency region gradually expands, and the low frequency region gradually lags behind, but there are still some exceptions: (1) at different temperatures, there is no consistent change rule in the high-frequency region; (2) at 45 °C, the initial real part impedance of the lithium battery with a maximum capacity of 0% is significantly larger

than that in other cases, and the overall hysteresis of the impedance line (see attention line of Fig. 2(c)) is more significant than that of the impedance line with the maximum capacity of 100%. Fig. 2(d)-(f) further supports the above conclusion. In Fig. 2(d)-(f), the decrease of RUL corresponds to the increase of real and negative imaginary parts impedance in the low frequency region and the middle frequency region. In the high frequency region, there is no corresponding rule, and at 45 °C, the situation is similar to that in Fig. 2(c) (see the attention line of Fig. 2(f) for details) at 45 °C. Fig. 3 shows the change of EIS impedance for all charge-discharge cycles of lithium battery, Fig. 3(a) and (b) show the variation of real and negative imaginary parts impedance, respectively. In Fig. 3, 9 cells in the first 100 discharge cycles, the change of real part impedance with charge-discharge cycles has a large uncertainty, and the individual battery and operating conditions will also have a greater impact on the change of real part impedance. In comparison, the battery's negative imaginary part impedance varies with battery cycling, with obvious regularity, the surge in negative imaginary part impedance shown in Fig. 3(b) generally occurs near the end of battery life. The surge in negative imaginary part impedance is caused by battery failure or near failure.

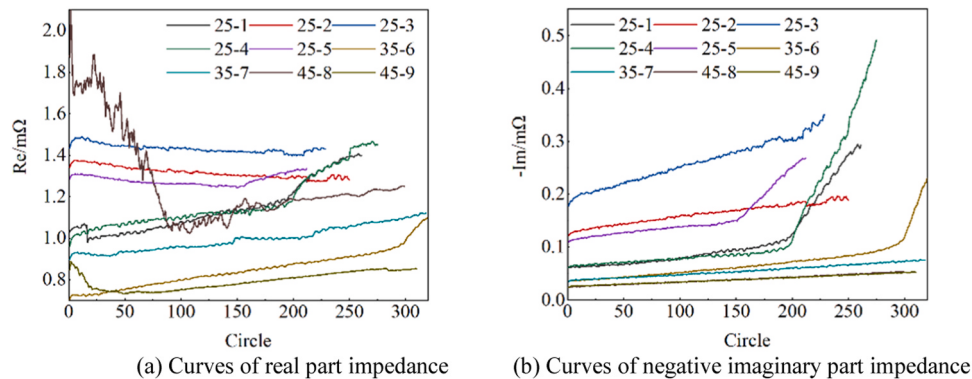


Fig. 3. The change of EIS impedance of lithium battery cycle.

2.2. Person correlation analysis

Assuming that the real and negative imaginary parts impedance data at different measurement frequencies are X , RUL is Y , and denoted as (X, Y) respectively, thus the correlation coefficient r is:

$$r = \frac{\sum_{i=1}^n (X_i - \bar{X})(Y - \bar{Y})}{\sqrt{\sum_{i=1}^n (X_i - \bar{X})^2} \sqrt{\sum_{i=1}^n (Y - \bar{Y})^2}} \quad (1)$$

where X_i is the real and negative imaginary parts impedance data collected at different frequencies, Y is the current RUL sequence and $n = 60$.

The Pearson correlation distribution is illustrated in Fig. 4. Fig. 4(a) and Fig. 4(b) show the Person correlation of real and negative imaginary parts impedance with RUL, respectively where f1-f60 represents 60 test frequencies, respectively.

It can be seen from Fig. 4 that the real part impedance data does not have obvious regularity at different temperatures, and the mapping relationship between real part impedance and RUL is greatly affected by temperature. In comparison, the mapping relationship between negative imaginary part impedance and RUL has relatively good regularity, especially when the frequency is f35-f60 (Fig. 4(b), attention area). The Pearson coefficients are all at different temperatures and all of them are close to -1 , which indicates that the negative imaginary part impedance at the corresponding frequency has a significant negative correlation with RUL, and is less affected by temperature.

3. RUL prediction model

Impedance data of 25-1, 25-2, 25-3, 35-6 and 45-8 is adopted as training set and impedance data of 25-4, 25-5, 35-7, and 45-9 is used as the test set in this study. The EIS impedance frequency range of the battery is 0.02 Hz-20 kHz, and a total of 60 frequencies have been studied. The impedance can be expressed as:

$$\begin{cases} Z' = [Z'_{01}, Z'_{02}, \dots, Z'_{60}] \\ Z'' = [Z''_{01}, Z''_{02}, \dots, Z''_{60}] \\ Z = Z' + jZ'' \end{cases} \quad (2)$$

where, Z'_i and Z''_i represent the battery real and negative imaginary parts impedance, respectively, and j represents the imaginary unit. Also, 1–60 represents the EIS frequency number of the impedance spectrum.

3.1. Data standardization

In order to fully extract the RUL information, the z-score method is used to normalize the EIS impedance data. The mean of the processed

data is 0 and the standard deviation is 1. The specific method is defined as

$$x* = \frac{x - \bar{x}}{\sigma} \quad (3)$$

where, x is the original data, \bar{x} is the mean of all the data, and σ is the standard deviation.

After the above processing, the EIS impedance data is defined as

$$\begin{cases} Z'_{norm} = \left[\frac{Z'_{01} - Z'_{m01}}{\sigma'_{01}}, \frac{Z'_{02} - Z'_{m02}}{\sigma'_{02}}, \dots, \frac{Z'_{60} - Z'_{m60}}{\sigma'_{60}} \right] \\ Z''_{norm} = \left[\frac{Z''_{01} - Z''_{m01}}{\sigma''_{01}}, \frac{Z''_{02} - Z''_{m02}}{\sigma''_{02}}, \dots, \frac{Z''_{60} - Z''_{m60}}{\sigma''_{60}} \right] \\ Z_{norm} = Z'_{norm} + Z''_{norm} \end{cases} \quad (4)$$

where, Z'_i and Z''_i represent the real and negative imaginary parts impedance of the battery, respectively, Z'_{mi} and Z''_{mi} , respectively represent the average value of the real and negative imaginary parts impedance of different cycles at the current frequency. Moreover, σ'_i , σ''_i represent the standard deviation of the real and negative imaginary parts impedance of different cycles at the current frequency, respectively. Also, Z'_{norm} and Z''_{norm} represent the normalized real and negative imaginary parts impedance arrays, respectively. After normalization, the discrimination of the data is increased, and the ability to represent the cycle number information is stronger.

3.2. Artificial neural network model

3.2.1. Summary of AM and SAM

Traditionally, a standard neural network can be viewed as a nonlinear transformation from an input to a fixed-dimensional latent representation. This paradigm brings difficulties to information flow control in neural networks and affects the final results (Song et al., 2020). Attention mechanism (AM) is used to solve this problem (Meb et al., 2021). AM can assign weights to input features, and improve the feature extraction ability of neural network models, thus alleviate the problem of neural network information overload to a certain extent. It is worth noting that there is a strong correlation between the data samples during the aging process of lithium batteries. However, AM only has a significant extraction effect on input features, which is obviously not enough to fully meet the needs of EIS impedance data feature extraction. To overcome shortcomings, this study considers the strong correlation between the CNN output and the network output labels. Therefore, based on the above discussion, this paper proposes a method of adding a self-attention layer after the network output layer and the CNN output layer, which improves the adaptive ability of artificial neural networks to the uncertainty of chaotic temporal input features.

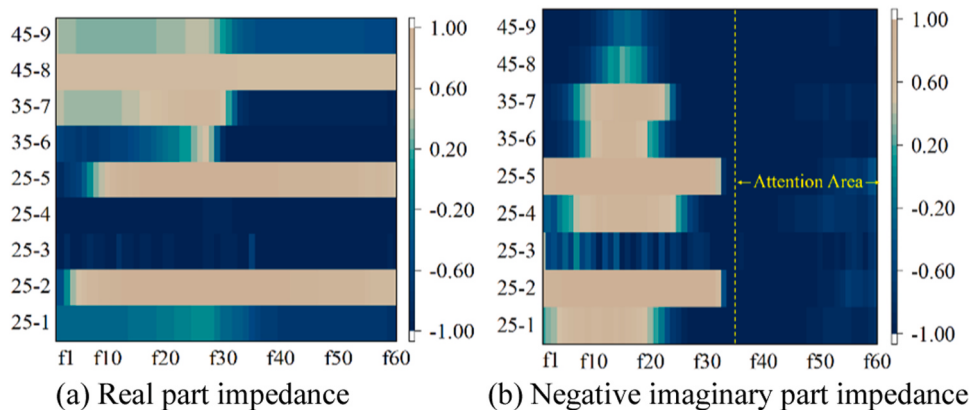


Fig. 4. Pearson correlation analysis of RUL impedance and RUL.

Fig. 5 shows the developed SAM structure. the self-attention structure proposed in this paper and c_1 is set as an example to indicate the calculation process of SAM. If the output of CNN is assumed to be $c = [c_1, c_2, \dots, c_n]$, taking c_i as an example, given a query vector $q_i = [q_{i1}, q_{i2}, \dots, q_{in}]$ and a key vector $k_j = [k_{j1}, k_{j2}, \dots, k_{jn}]$. Therefore, the similarity score between q_i and each k_j can be calculated by the Scaled-Dot-Product function shown in Eq. (5), where d is the dimension value of the output of the CNN layer. Then it is normalized to $[0,1]$ by the soft-max function, which can be shown in Eq. (6). Finally, the corresponding weight representation of c_i can be obtained as shown in Eq. (7). Finally, the parameter c'_i , which is updated by c_i weighting, can be expressed as Eq. (8).

In the above calculation process, the calculation process of the given q_i , k_j and v_i can be shown in Eq. (9). It can be seen from Eq. (6) to Eq. (9) that, a series of computations of SAM is differentiable. That is, W_Q , W_K and W_V are the parameter matrices that the neural network can learn during the end-to-end training process. Without loss of generality, according to the calculation process of Eq. (6) to Eq. (9), the remaining weighted CNN output values can be obtained as follows :

$$\alpha_{ij} = \frac{q_i k_j}{\sqrt{d}} \quad (j = 1, 2, 3, \dots, n) \quad (5)$$

$$\hat{\alpha}_{ij} = \frac{e^{\hat{\alpha}_{ij}}}{\sum_{i=1}^n e^{\hat{\alpha}_{ij}}} \quad (j = 1, 2, 3, \dots, n) \quad (6)$$

$$a_i = \sum_{j=1}^n \hat{\alpha}_{ij} v_j \quad (j = 1, 2, 3, \dots, n) \quad (7)$$

$$c'_i = c_i a_i \quad (8)$$

$$\begin{cases} q_j = c_j W_Q \\ k_j = c_j W_K \quad (j = 1, 2, 3, \dots, n) \\ v_j = c_j W_V \end{cases} \quad (9)$$

3.2.2. Fusion model Conv1d-SAM

This paper takes the negative imaginary part impedance of the electrochemical impedance spectrum as the input, and each set of inputs has 60 features. Since the established lithium battery RUL prediction model required in this study does not rely on any historical data of the lithium battery, the prediction can be completed using the currently measured EIS impedance spectrum. Accordingly, this paper proposes a fusion model Conv1d-SAM to extract RUL features in EIS impedance data, and its architecture is shown in Fig. 6. It starts with stacked convolutional and max-pooling layers that can extract features and compress the information in the form of feature maps. Then the output of CNN is connected to the SAM layer, and the CNN output is updated by taking advantage of the weight distribution advantage of SAM. Subsequently, three dense layers are concatenated to further increase the capacity of the CNN. The last layer outputs the predicted RUL value.

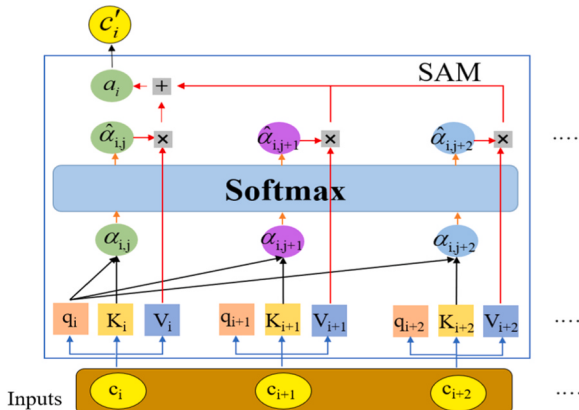


Fig. 5. The structure of SAM.

Set the size of the four-layer convolution kernel as 1×10 , 1×6 , 1×6 , and 1×3 , the number of convolution kernels is 80, the convolution step size is 1, the filling method adopts the same filling method, and the activation function is linear. The pooling process adopts the method of maximum pooling, the size of the pooling layer and the pooling step size is set to 1×2 and 1, respectively. The number of neurons in SAM is 80. After flattening the output of the updated CNN layer, it is connected to three fully connected layers. The number of neurons is 128, 64 and 1, respectively. The activation function is linear. Table 1 shows the model structure.

In this study, Adam algorithm is used for parameter optimization in the back-propagation process of network training during the training process. Adam algorithm is a commonly used optimization algorithm. Compared with the traditional gradient descent algorithm, the Adam algorithm combines the advantages of the Momentum and the RMSprop algorithms. That is, the exponentially weighted average of the gradient is calculated, and the weight w and the bias b are updated with the gradient, which reduces the longitudinal fluctuation in the optimization process, increases the optimization speed, and improves the training efficiency.

The loss function is the mean absolute error (MAE) function which is defined as follows:

$$MAE = \frac{1}{N} \sum_{i=1}^N |y_i - \hat{y}_i| \quad (10)$$

3.2.3. Model evaluation

The root mean square error (RMSE), mean absolute error (MAE), and R^2 are adopted as evaluation indicators to evaluate the trained model. The calculation methods of each of the above parameters are calculated as follows:

$$RMSE = \sqrt{\frac{1}{N} \sum_{i=1}^N (y_i - \hat{y}_i)^2} \quad (11)$$

$$MAE = \frac{1}{N} \sum_{i=1}^N |y_i - \hat{y}_i| \quad (12)$$

$$R^2 = \frac{\left(N \sum_{i=1}^N y_i \hat{y}_i - \sum_{i=1}^N y_i \sum_{i=1}^N \hat{y}_i \right)^2}{\left(N \sum_{i=1}^N \hat{y}_i^2 - \left(\sum_{i=1}^N \hat{y}_i \right)^2 \right) \left(N \sum_{i=1}^N y_i^2 - \left(\sum_{i=1}^N y_i \right)^2 \right)} \quad (13)$$

where, N is the number of samples, y_i is the real value RUL value, and \hat{y}_i is the predicted RUL value. When the predicted value is closer to the true value, the smaller the values of MAE and RMSE, the larger the R^2 value. That is, the smaller the error, the higher the fitting degree, and the higher the accuracy of the model.

4. Analysis of results

The EIS impedance spectroscopy data were collected in the V state. The end of life (EOL) of a lithium battery is defined as the number of used cycles of a lithium battery when the battery capacity is 80% lower than its initial value. EOL values of 25–4, 25–5, 35–7 and 45–9 are 150 and 252, 252 and 396 cycles, respectively.

In this study, RUL of different batteries of the same type (25–4 and 25–5) is predicted at the same temperature, and then RUL of batteries (25–4, 35–7 and 45–9) is predicted at different operating temperatures. Furthermore, MLP, Conv1d, Conv2d and EIS-GPR are designed as the competition models to verify the performance of the proposed model. The analysis and verification is carried out from the perspectives of the experimental frequency and the prediction model, respectively.

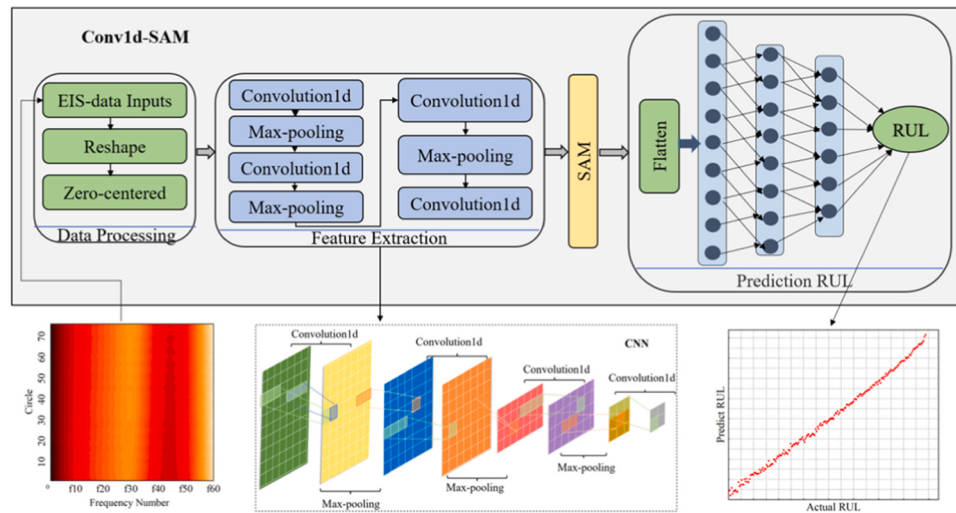


Fig. 6. The structure of Conv1d-SAM.

Table 1
THE STRUCTURE OF CONV1D-SAM AFTER TRAINING.

Layer	Output Shape	Parameter
Conv1D	(None, 60, 80)	880
MaxPool1D	(None, 30, 80)	0
Conv1D	(None, 30, 80)	38480
MaxPool1D	(None, 15, 80)	0
Conv1D	(None, 15, 80)	38480
MaxPool1D	(None, 7, 80)	0
Conv1D	(None, 7, 80)	19280
SAM	(None, 80)	6400
Flatten	(None, 80)	0
Dense	(None, 128)	10368
Dense	(None, 64)	8256
Dense	(None, 1)	65

4.1. Analysis and verification of test frequency and impedance data

The above studies prove that real part impedance is greatly affected by temperature, and the mapping relationship between negative imaginary part impedance and RUL shows obvious regularity when the frequency is f35-f60. Therefore, in order to fully validate the proposed method, the impedance data obtained at 60 measurement frequencies (120 in total, labeled as q1-q120) are divided into four groups as input features to train the model: the first group is the real and negative imaginary parts impedance data measured at 60 frequencies. The second group is the real part impedance data (q1-q60). The third group is the negative imaginary part impedance data at 60 frequencies (q61-q120). The fourth set of data is the negative imaginary part impedance data (q95-q120) at frequencies from 35 to 60 determined by Pearson correlation analysis. With the above four groups of features as input, the proposed Conv1d-SAM and Conv2d networks were used to predict RUL.

Fig. 7 shows the prediction results of Conv1d-SAM for three different batteries when the above four sets of features are used as model inputs separately. Table 2 shows the comparison of the prediction results.

Notice that the prediction effect of RUL at different frequencies has a

The fourth set of data is the negative imaginary part impedance data (q95-q120) at frequencies from 35 to 60 determined by Pearson correlation analysis. With the above four groups of features as input, the proposed Conv1d-SAM and Conv2d networks were used to predict RUL. Fig. 7 shows the prediction results of Conv1d-SAM for three different batteries when the above four sets of features are used as model inputs separately. Table 2 shows the comparison of the prediction results.

Table 2
Comparison of prediction results of four input features.

Features	CELL	Conv1d-SAM			Conv2d		
		R ²	MAE	RMSE	R ²	MAE	RMSE
q1-q120	25-4	0.97	5.59	7.15	0.87	9.31	12.10
	25-5	0.97	5.1	6.16	0.76	9.78	12.20
	35-7	0.95	14.14	16.03	0.93	13.96	16.66
	45-9	0.99	8.72	9.92	0.52	49.25	56.62
	q1-q60	0.82	15.76	18.74	0.55	28.35	29.40
	25-5	0.82	12.07	14.81	0.55	23.12	23.12
	35-7	0.07	59.73	70.73	-1	97.90	103.74
	45-9	0.62	56.69	71.15	0.76	47.73	55.14
	q61-q120	0.97	5.97	7.35	0.93	8.59	11.34
	25-5	0.98	4.12	5.29	0.91	9.20	10.11
	35-7	0.98	8.00	10.96	0.94	12.55	14.55
	45-9	0.99	6.41	8.11	0.99	6.27	8.39
q95-q120	25-4	-1.94	74.27	75.22	-2	78.02	79.68
	25-5	0.48	17.76	25.30	-0.73	43.94	46.37
	35-7	0.91	19.33	21.82	0.55	46.62	48.98
	45-9	0.97	15.12	18.19	0.98	11.42	13.64

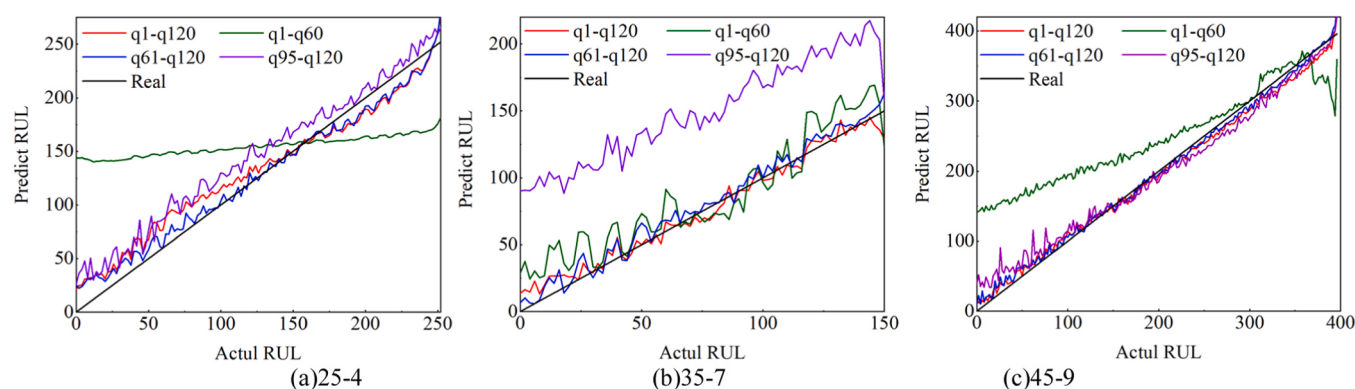


Fig. 7. Comparison of prediction results of Conv1d-SAM at different frequencies.

great relationship with the individual battery and operating temperature. However, when q61-q120 and q1-q120 are used as input features, they have relatively good prediction results under different battery individuals and operating temperatures. Especially, the best results are obtained when q61-q120 is the input features. The possible reason is that real part impedance information of q1-q120 is greatly affected by temperature, thus effective real part impedance information is difficult to obtain. When q95-q120 is employed as the characteristic inputs, the prediction performance for 25–4 battery RUL is poor. This indicates that q95-q120 contains less aging information of lithium batteries, which is not conducive to the deep extraction of aging information from EIS data.

Note that when q61-q120 is used as the input feature, both Conv1d-SAM and Conv2d models have better prediction results, and MAE of their prediction results at different temperatures is less than or equal to 8. The above analysis confirms that q61-q120 is more suitable as the input feature.

4.2. Comparative study of different neural network models

With q61-q120 as input feature, the RUL was predicted by conv1d-sam, MLP, Conv1d, Conv2d and EIS-GPR (Zhang et al., 2020). The parameters of MLP, Conv1d, and Conv2d are all combinations of optimal values selected after multiple experiments. The predictions of Conv1d-SAM and its competing models for 25–4, 25–5, 35–7, and 45–9 batteries are shown in Fig. 8. The abscissa represents the real RUL value, and the ordinate represents the predicted RUL value. R^2 in the lower right corner of the figure is the evaluation index of Conv1d-SAM.

Conv1d-SAM can better capture the detailed changes at the end of battery life and reduce the prediction error at the end of battery life under the experimental environment. Compared with other competing models, it has obviously better prediction accuracy and stability. This shows that the negative imaginary part impedance contains relatively complete battery cycle aging information, and Conv1d-SAM model can effectively extract aging features from EIS data.

Fig. 9 shows the comparison of Conv1d-SAM with the evaluation indicators of the prediction results of the competition model. Table III summarizes the evaluation indicators of the prediction results. It can be seen from Table 3 that the R^2 values of Conv1d-SAM are all higher than 0.97 at three temperatures, and MAE values are all less than 8. Compared with EIS-GPR (Zhang et al., 2020), MLP, Conv1d and Conv2d, MAE values are increased by 72%, 48%, 57%, and 33.6%, respectively.

5. Conclusion

According to the EIS impedance spectrum characteristics of lithium battery at different temperatures, a lithium battery RUL prediction method based on EIS-IM-Conv1d-SAM fusion neural network is proposed in this study. The following conclusions are obtained.

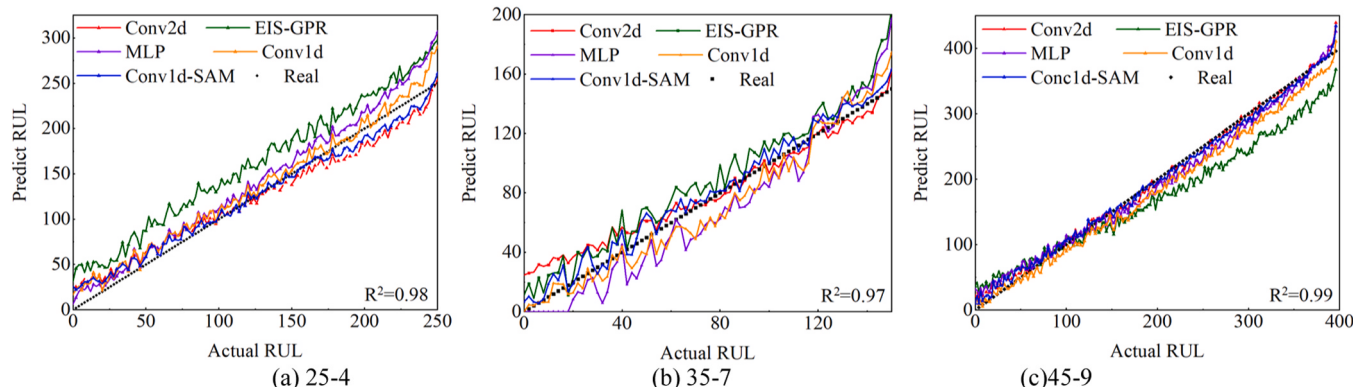


Fig. 8. Prediction results comparison of different models.

- (1) The negative imaginary part impedance of lithium batteries increases significantly with the aging of battery, especially in the medium frequency band of the EIS impedance spectrum, and it is not dependence on operation temperature, while the real part impedance shows a strong correlation with battery temperature. In addition, it is found that the negative imaginary part impedance of EIS can map the RUL of lithium battery.
- (2) The neural network has the best generalization performance in RUL prediction when the EIS negative imaginary part impedance of 60 frequencies are used as input features. Furthermore, compared with the traditional RUL prediction method, the proposed method is more suitable for online RUL prediction without relying on the historical charging and discharging cycle information of lithium batteries.
- (3) Compared with MLP, Conv1d and Conv2d, the proposed fusion model of EIS-IM-Conv1d-SAM integrates the advantages of CNN and SAM, and can more fully mine the battery RUL information contained in the negative imaginary part impedance data of EIS, with better accuracy and stability. Compared with the current optimal method (EIS-GPR), MAE of EIS-IM-Conv1d-SAM was improved by 72%.

In this paper, the prediction of battery RUL was realized based on the measured data of electrochemical impedance spectroscopy. This research was only conducted on lithium batteries within the life cycle of conventional operating conditions. The prediction of the impedance variation characteristics of lithium batteries during the life cycle caused by the abuse of lithium batteries and the RUL prediction of abnormal cells of battery pack temperature are the follow-up research direction.

Funding

This work was supported by the Key Research and Development Program of Shaanxi Province under Grant 2022GY-178, the Science and Technology Program Project of Chinese State Administration for Market Regulation (SAMR) under Grant 2021MK104, the International Innovation Project of Shaanxi Province under Grant S2022-ZC-GXYZ-0015, and the Ministry of Science and Technology of China under Grant G2021171024L.

Author statement

We would like to thank you for spending valuable time and encouraging us to resubmit our manuscript after refining it following the reviewers suggestions, and also thank for the reviewers' comments concerning our manuscript entitled "Remaining Useful Life Prediction of Lithium-ion Batteries via an EIS Based Deep Learning Approach". Those comments are all valuable and very helpful for revising and improving our paper, as well as the important guiding significance to our

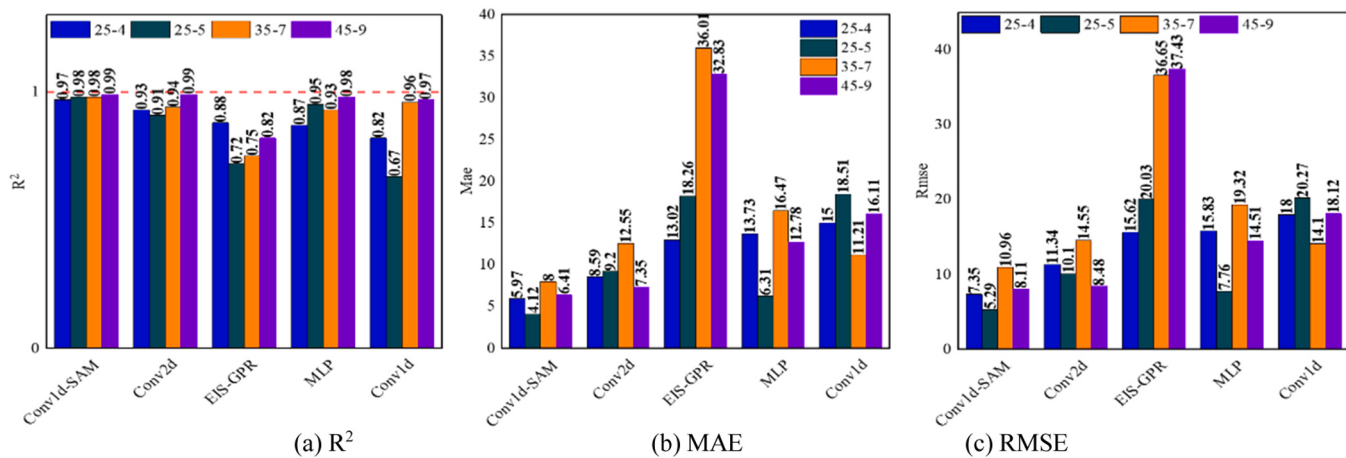


Fig. 9. Comparison of evaluation parameters.

Table 3
Evaluation Indicators of Different Models.

Models	CELL	R ²	MAE	RMSE
Conv1d-SAM	25-4	0.97	5.97	7.35
	25-5	0.98	4.12	5.29
	35-7	0.98	8.00	10.96
	45-9	0.99	6.41	8.11
Conv2d	25-4	0.93	8.59	11.34
	25-5	0.91	9.19	10.10
	35-7	0.94	12.55	14.55
	45-9	0.99	7.34	8.48
EIS-GPR	25-4	0.88	13.02	15.62
	25-5	0.72	18.26	20.03
	35-7	0.75	36.01	36.65
	45-9	0.82	32.82	37.43
MLP	25-4	0.87	13.73	15.83
	25-5	0.95	6.31	7.76
	35-7	0.93	16.47	19.32
	45-9	0.98	12.78	14.51
Conv1d	25-4	0.82	15.00	18.00
	25-5	0.67	18.51	20.27
	35-7	0.96	11.21	14.10
	45-9	0.98	16.11	18.12

researches. We have studied all issues mentioned in the reviewers' comments carefully, however, we found that reviewers 3' comments are not for our paper, which out are not relevant to our research. We have provided a detailed explanation of the specific reasons in the letter of Response to Reviewers. We hope to receive your response to this issue. Thank you again for your work.

Declaration of Competing Interest

The authors declare that they have no known competing financial interests or personal relationships that could have appeared to influence the work reported in this paper.

Data availability

The authors do not have permission to share data.

References

- Agudelo, B., Zamboni, W., Monmasson, E., et al., 2019. Identification of battery circuit model from EIS data. JCGE-Congrès Des. Jeunes Cherch. En. Génie Électr.
- Babaeiyazdi, I., Rezaei-Zare, A., Shokrzadeh, S., 2021. State of charge prediction of EV Li-ion batteries using EIS: a machine learning approach. Energy 223, 120116.
- Birk, C.R., Roberts, M.R., McTurk, E., et al., 2017. Degradation diagnostics for lithium ion cells. J. Power Sources 341 (11), 373–386.
- Bohlen, O., Kowal, J., Sauer, D.U., 2007. Ageing behaviour of electrochemical double layer capacitors: Part I. Experimental study and ageing model. J. Power Sources 172 (1), 468–475.
- Broussely, M., Biensan, P., Bonhomme, F., et al., 2005. Main aging mechanisms in Li ion batteries. J. Power Sources 146 (1–2), 90–96.
- Chen, L., Wang, H., Chen, J., et al., 2020. A novel remaining useful life prediction framework for lithium-ion battery using grey model and particle filtering. Int. J. Energy Res. 44 (9), 7435–7449.
- Deng, Z., Hu, X., Lin, X., et al., 2020. Data-driven state of charge estimation for lithium-ion battery packs based on Gaussian process regression. Energy 205, 118000.
- Dong, G., Chen, Z., Wei, J., et al., 2018. Battery health prognosis using brownian motion modeling and particle filtering. IEEE Trans. Veh. Technol. 65 (11), 8646–8655.
- Eddahech, A., Briat, O., Woigard, E., et al., 2012. Remaining Useful Life prediction of Lithium batteries in calendar ageing for automotive applications. Microelectron. Reliab. 52 (9–10), 2438–2444.
- Guha, A., Patra, A., 2018. State of health estimation of lithium-ion batteries using capacity fade and internal resistance growth models. IEEE Trans. Transp. Electrification 4 (1), 135–146.
- Hu, X., Li, S., Peng, H., 2012. A comparative study of equivalent circuit models for Li-ion batteries. J. Power Sources 198, 359–367.
- Li D., Yang L. Remaining useful life prediction of lithium battery using convolutional neural network with optimized parameters[C], in 2020 5th Asia Conference on Power and Electrical Engineering (ACPEE), Chengdu, China, June. 2020, pp.840–844.
- Li, W., Jiao, Z., Du, L., et al., 2019. An indirect RUL prognosis for lithium-ion battery under vibration stress using elman neural network. Hydrot. Energy 44 (23), 12270–12276.
- Meb, A., Sn, A., Ma, B., et al., 2021. ABCDM: an attention-based bidirectional CNN-RNN deep model for sentiment analysis. Future Gener. Comput. Syst. 115 (5), 279–294.
- Messing M., Shoa T., Ahmed R., et al. Battery SoC Estimation from EIS using Neural Nets [C], in 2020 IEEE Transportation Electrification Conference & Expo (ITEC). Chicago, IL, USA, June 2020, pp.588–593.
- Messing M., Shoa T., Habibi S., EIS from Accelerated and Realistic Battery Aging[C], in 2021 IEEE Transportation Electrification Conference & Expo (ITEC), Chicago, IL USA, June, 2021: pp.720–725.
- Monika, K., Julia, B., Moritz, H., Kuebra, K., et al., 2018. Determination of SoH of lead-acid batteries by electrochemical impedance spectroscopy. Appl. Sci. 8 (6), 1–5.
- Murariu, T., Morari, C., 2019. Time-dependent analysis of the state-of-health for lead-acid batteries: An EIS study. J. Energy Storage 21 (11), 87–93.
- Pastor-Fernández C., Dhammadka Widanage W., Marco J., et al. Identification and quantification of ageing mechanisms in Lithium-ion batteries using the EIS technique [C], in 2016 IEEE Transportation Electrification Conference and Expo (ITEC), Dearborn, USA, June 2016, pp. 1–6.
- Ramadass, P., Haran, B., White, R., et al., 2003. Mathematical modeling of the capacity fade of Li-ion cells. J. Power Sources 123 (2), 230–240.
- Saha, B., Goebel, K., Poll, S., et al., 2009. Prognostics methods for battery health monitoring using a bayesian framework. IEEE Trans. Instrum. Meas. 58 (2), 291–296.
- Shen, D., Xu, T., Wu, L., et al., 2019. Research on degradation modeling and life prediction method of lithium-ion battery in dynamic environment. IEEE Access 7 (9), 130638–130649.
- Song, G., Wang, Z., Han, F., et al., 2020. Music auto-tagging using scattering transform and convolutional neural network with self-attention. Appl. Soft Comput. 96 (106702), 1–8.
- Sun, B., Pan, J., Wu, Z., et al., 2023. Adaptive evolution enhanced physics-informed neural networks for time-variant health prognosis of lithium-ion batteries. J. Power Sources 556, 1–12.
- Sun, T., Xia, B., Liu, Y., et al., 2019. A novel hybrid prognostic approach for remaining useful life estimation of lithium-ion batteries. Energies 12 (9), 1–22.

- Sun, Y., Hao, X., Pecht, M., Zhou, Y., 2018. Remaining useful life prediction for lithium-ion batteries based on an integrated health indicator. *Microelectron. Reliab.* 88 (90), 1189–1194.
- Vetter, J., Novák, P., Wagner, M.R., et al., 2005. Ageing mechanisms in lithium-ion batteries. *J. Power Sources* 147 (1–2), 269–281.
- Wang, F., Mamo, T., 2018. A hybrid model based on support vector regression and differential evolution for remaining useful lifetime prediction of lithium-ion batteries. *J. Power Sources* 401 (73), 49–54.
- Wu J., Xu J., Huang X..An indirect prediction method of remaining life based on glowworm swarm optimization and extreme learning machine for lith[C], in 2017 36th Chinese Control Conference (CCC), Dalian, China, July.2017, pp.7259–7264.
- Xia F., Yuan B., Peng D., et al. Modeling and Optimization of Variable-order RC Equivalent Circuit Model for Lithium-ion Batteries Based on Information Criterion [J]. Proceedings of the CSEE, 2018,38(21), pp. 49–54.
- Xiong, R., Zhang, Y., Wang, J., et al., 2019. Lithium-ion battery health prognosis based on a real battery management system used in electric vehicles. *IEEE Trans. Veh. Technol.* 68 (5), 4110–4121.
- Yang, J., Xia, B., Huang, W., et al., 2018. Online state-of-health estimation for lithium-ion batteries using constant-voltage charging current analysis. *Appl. Energy* 212 (15), 1589–1600.
- Zhang, Y., Tang, Q., Zhang, Y., et al., 2020. Identifying degradation patterns of lithium-ion batteries from impedance spectroscopy using machine learning. *Nat. Commun.* 11 (1), 1–6.
- Zhou B., Cheng C., Ma G., et al. Remaining Useful Life Prediction of Lithium-ion Battery based on Attention Mechanism with Positional Encoding[C], in IOP Conference Series Materials Science and Engineering, Tokyo, Japan,Jan.2020.
- Zhou D., Song X., Lu W., et al. Research on real-time assessment method of lithium battery health status based on daily segment charging data[J], Proceedings of the CSEE, 2019,39(1), pp. 105–111.
- Zhu, J.G., Sun, Z.C., Wei, X.Z., et al., 2015. A new lithium-ion battery internal temperature on-line estimate method based on electrochemical impedance spectroscopy measurement. *J. Power Sources* 274, 990–1004.
- Zou, Y., Li, S., et al., 2016. State-space model with non-integer order derivatives for lithium-ion battery. *Appl. Energy* Barking Then Oxf. 161, 330–336.